



Removal of chromium from synthetic wastewater by adsorption onto Ethiopian low-cost Odaracha adsorbent

Yohanis Birhanu¹ · Seyoum Leta² · Getachew Adam³

Received: 24 February 2020 / Accepted: 2 October 2020 / Published online: 16 October 2020
© The Author(s) 2020

Abstract

Nowadays, Cr-loaded wastewater released from industrial activities pose an increasing risk to human health and the environment. Adsorption processes have been widely used for the removal of chromium from the waste stream. In this regard, natural adsorbents are the most preferable and cost-effective methods. In this study, the efficiency of Odaracha adsorbent as a novel green technology in the removal of chromium from synthetic wastewater is analyzed. Batch adsorption experiments were conducted to evaluate the effect of contact time, pH, adsorbent dose, and initial concentration of adsorbate on Cr removal. The surface morphology of Odaracha adsorbent was characterized by scanning electron microscopy, Fourier transform infrared spectroscopy, and X-ray powder diffraction. Experimental results showed that Odaracha adsorbent could perform effectively in a wide range of experimental conditions. However, in optimum experimental conditions, such as 180-min contact time, pH 3, and 15 g/L of adsorbent dose Odaracha adsorbent removes 94.68% of Cr from an aqueous solution having 110 mg/L of Cr concentration.

Keywords Odaracha · Synthetic wastewater · Chromium · Adsorption

Introduction

Metals are ubiquitous in the environment because of their wide application (Ajmani et al. 2019b). They are present in the solid phase and solution, as free ions, or adsorbed to colloidal soil particles. From these metals, hexavalent chromium has no known vital or beneficial effect on organisms, even for bacterial cells, and its accumulation over time in organisms can cause serious illness even at low concentration. According to World Health Organization (WHO) guidelines, the allowable concentration of Cr (VI) in drinking water is 50 ppb (Jiang et al. 2013). However, humans could be exposed to higher-level chromium

contamination through food or drinking water. Industries such as leather tanning, steel fabrication, metal finishing, and other industrial sources related to wood preservation are the major causes of this contamination (Eliku and Leta 2018). The human health effects of hexavalent chromium exposure are respiratory irritation, dermatitis, lung cancer, kidney, and liver damage (Ofudje et al. 2014; Jiang et al. 2013). Therefore, the removal of Cr would be necessary to improve the quality of water and the life of humanity. In line with minimizing the adverse effect on human health nowadays, there are several Cr removal mechanisms. For the removal of chromium from wastewater, adsorption is highly effective compared to other conventional methods (Pranay et al. 2015; Shahnaz et al. 2020b). Adsorption is a process that occurs when a gas or liquid or solute (called adsorbate) accumulates on the surface of a solid or more rarely a liquid (adsorbent), forming a molecular or atomic film. Adsorption process can be influenced by a number of factors such as pH, adsorbate concentration, adsorbent dosage, and other factors (Costanzo et al. 2012).

Most clay can soak up electrically charged atoms and molecules from the solution. Clays' mineral composition, crystal structural characteristics, and their crystalline size make them potentially sound absorbers (Hoidy et al. 2009).

✉ Yohanis Birhanu
yohanis.birhanu@aau.edu.et

¹ Department of Chemistry, College of Natural and Computational Science, Jigjiga University, P.O. Box 1020, Jigjiga, Ethiopia

² Center of Environmental Science, Addis Ababa University, P.O. Box 1176, Addis Ababa, Ethiopia

³ Department of Industrial Chemistry, Center of Excellence in Sustainable Energy, Addis Ababa Science and Technology University, P.O. Box 16417, Addis Ababa, Ethiopia

Besides, because of their availability and cost-effectiveness, clay minerals become the most critical industrial resource. As a result, clays have received considerable attention, especially as potential adsorbents for environmental research. In line with the adsorption potential of clay mineral, in the eastern part of Ethiopia, specifically in Saketa district, there is a clay locally named Odaracha. In most of the rural areas of West Hararghe zone of Oromia, regional state peoples depend on this particular kind of clay (Odaracha clay) to remove turbidity of water in their day-to-day life and commercially exchanged in the market for this particular purpose in some woredas. Odaracha soil is a novel adsorbent material and has not been reported in the literature. Therefore, the principal aim of this study was to investigate the effectiveness of Odaracha clay in the removal of Cr from synthetic wastewater. The effect of various parameters such as contact time, pH, adsorbent dose, and initial concentration of adsorbate on adsorption efficiency of Odaracha was considered.

Materials and methods

Chemicals and analytical methods

The chemicals consumed in these set of experimental activities were all of analytical grade. The standard stock solution of chromium (1000 mg/L) was prepared by dissolving 2.828 g of 99.9% analytical-grade $K_2Cr_2O_7$ in 1000 mL of distilled water. All the required solutions are made ready with analytical-grade reagents and double-distilled water. Synthetic samples of different concentrations of chromium are prepared from this stock solution by appropriate dilutions. The functional groups involved in the adsorption process were identified by Fourier transform infrared (FTIR) spectroscopy (Model 65 spectrometer, USA). X-ray powder diffraction analysis was performed using the XRD spectrometer (PAN analytical X'Pert Pro) with recorded 2θ XRD patterns of 5° to 60° . The surface morphology of Odaracha adsorbent was characterized using INSPECT F50 field emission scanning electron microscope (SEM).

Adsorbent preparation

In this study, a locally available soil type, known by the local community as Odaracha clay, was used as an adsorbent. This natural coagulant is abundantly available in Saketa District West Hararghe zone of Oromia Regional State, Ethiopia. It is also commercially exchanged in the market of Boke Tiko woreda, and the rural communities have been using this clay material to remove water turbidity. In this research, the soil sample was taken from Saketa district (N: $08^\circ 44' 41.3''$ E: $040^\circ 45' 15.1''$, altitude 1470). After air-dried, the soil has

been crushed into the desired size and sieved using 125- μ m laboratory sieve. Finally, Odaracha powder was dried in the oven with a $120^\circ C$ temperature level for 6 h and kept inside the desiccator until the adsorption experiment.

Batch adsorption experiments

The batch adsorption studies were conducted at room temperature by agitating measured quantities of the Odaracha adsorbent in 50 ml of synthetic wastewater at the rate of 150 rpm with the required pH, contact time, dose of the adsorbent and initial concentration of the adsorbate. The timing was started upon the addition of adsorbent. These experiments were run in different Erlenmeyer flasks having a capacity of 150 ml. After shaking, the sample was taken and filtered by the Whatman membrane filter paper of pore size 0.45 μ m. Finally, the sample was analyzed by FAAS (Flame Atomic Absorption Spectrophotometer, Model 210 VGP) for the remaining chromium ion in the solution. The experiments were undertaken in triplicate, and the average results are presented. The removal efficiencies of Odaracha adsorbent were investigated based on the following equations. The percentage of chromium removal is obtained using Eq. 1, while the adsorption capacity q_e is calculated using Eq. 2.

$$\% \text{removal} = \frac{(C_o - C_e)}{C_o} \times 100 \quad (1)$$

where C_o = initial adsorbate concentration (mg/L); C_e = final equilibrium adsorbate concentration (mg/L).

$$q_e = \frac{(C_o - C_e)V}{w} \quad (2)$$

where C_o and C_e are the initial and equilibrium liquid-phase concentrations of the Cr ions in mgL^{-1} , respectively, V is the volume of the solution in L, w is the amount of adsorbent used in g, and q_e is the removal efficiency of adsorbent in mg/g .

Isotherm and kinetic studies

To study the adsorption isotherms, the optimum conditions found in optimization experiments were applied only by varying adsorbent doses. These experiments were carried out using adsorbent dose in the range of 1, 3, 5, 7, 10, 15, and 20 g/L. For each adsorbent dosage, 50 ml of the sample was taken and agitated at 150 rpm. The data from the experiment were fitted into Langmuir and Freundlich adsorption isotherm models (Gulipalli et al. 2011). It is essential to know the rate at which the process takes place, factors that control the rate of the process; for this reason, the kinetics of the processes were assessed. These experiments were

conducted by setting heavy metal concentration, pH, adsorbent dosage, and agitation speed constant. Then, the sample was withdrawn at 30, 60, 90, 120, 150, 180, and 210 min for the determination of residual heavy metals in the solution. Then, data from the experiment were introduced into the pseudo-first-order model of Lagergren and pseudo-second-order models of Ho and McKey (Dagmawi and Mekibib 2013; Gulipalli et al. 2011).

Results and discussion

Characterization of Odaracha adsorbent

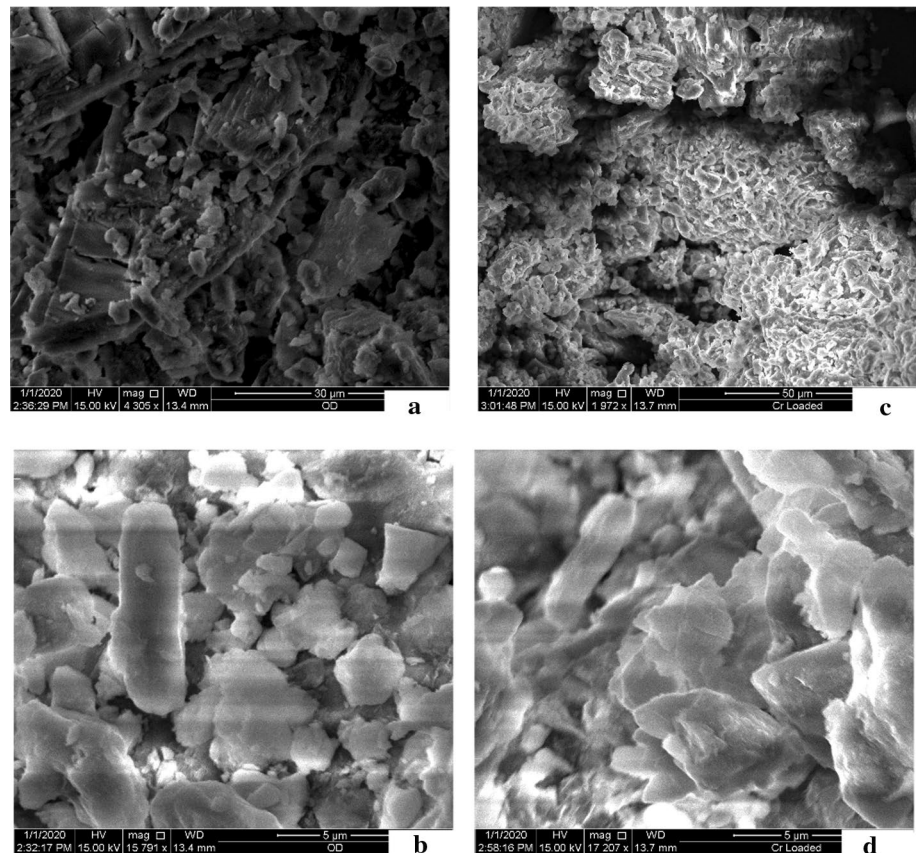
Scanning electron microscope (SEM) studies

The scanning electron microscope (SEM) images shown in Fig. 1 revealed the surface morphology of Odaracha adsorbent before and after adsorption. As shown in Fig. 1a, b Odaracha adsorbent appears rough and porous before adsorption. However, as depicted in Fig. 1c, d, the morphology of Odaracha adsorbent after Cr adsorption appears different where the pores are filled and much smoother. This is an indication of the adsorption of Cr onto the surface of Odaracha adsorbent.

FTIR studies

The FTIR spectra of Odaracha clay are shown in Fig. 2. The spectra in the region $3200\text{--}3650\text{ cm}^{-1}$ and the maximum peak 3408 cm^{-1} were due to --OH stretching vibration. The strong peaks at 2519 , 1432 , and 1038 cm^{-1} were due to O--H (carboxylic acid) stretching, C--O , and Si--O--Si (organic siloxane or silicone) bond, respectively (Ghoneim et al. 2014; Kyziol-Komosinska et al. 2014). The spectra viewed below 1000 cm^{-1} are more comparable to the mineral features of the material. To identify the possible functional groups on Odaracha adsorbent involved in the binding of Cr, FTIR spectra were obtained before and after adsorption. If a ligand coordinates to a metal, the ligand material's energy will most likely be disturbed, leading ultimately to shifts in the absorption peaks in the FTIR spectra. These FTIR adsorption bands are ordinarily shifted to lower or upper frequencies. In this regard, there are small shifts of vibration from 873 , 1038 , 2131 , 2519 , 2874 , and 3408 cm^{-1} in Odaracha adsorbent to 872 , 1027 , 2127 , 2518 , 2870 , 3408 cm^{-1} for chromium-loaded adsorbent, respectively. The disappearance of intensities and shifting of peaks to new values signify the involvement of functional groups in the adsorption process.

Fig. 1 SEM images of Odaracha adsorbent before adsorption (a, b) and after adsorption (c, d)



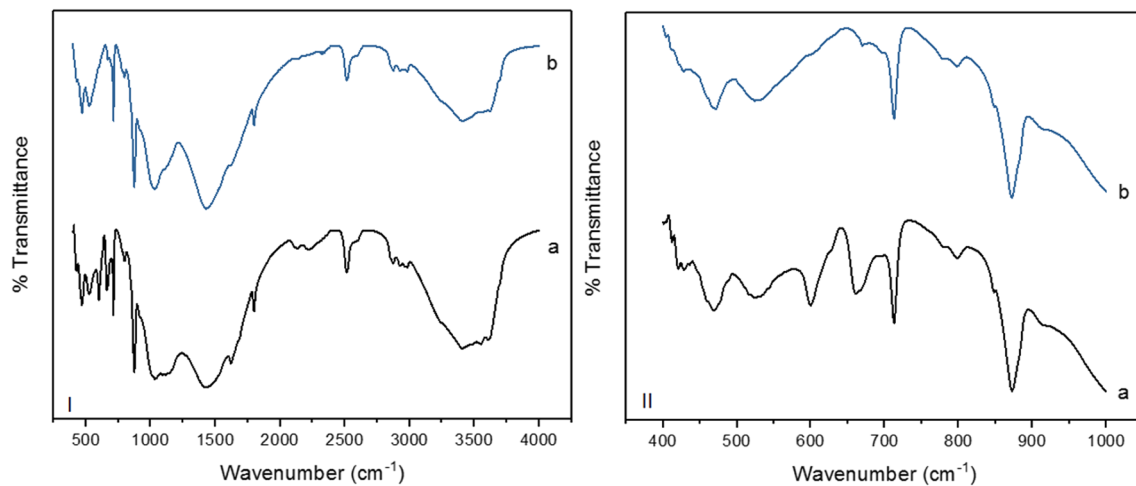


Fig. 2 FTIR spectrum (400–4000 cm^{-1} (I) and 400–1000 cm^{-1} (II)) of raw (a) and chrome-loaded (b) Odaracha powder

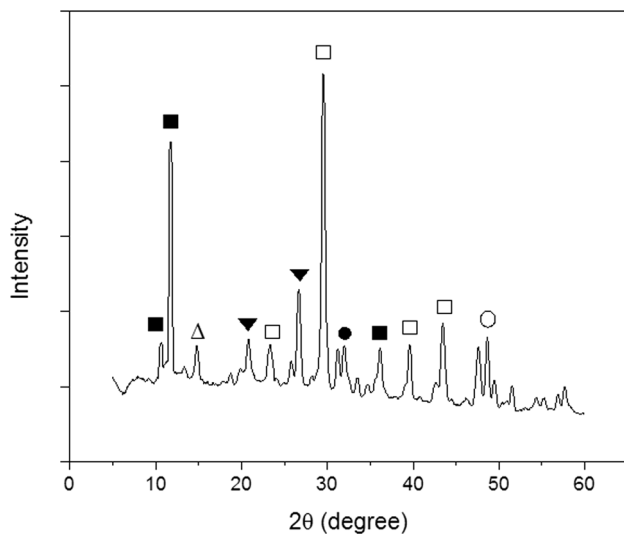


Fig. 3 X-ray diffraction patterns of raw Odaracha clay. Mineral assignments: gypsum (■), alumina (Δ), quartz (▼), calcite (□), dolomite (●) and magnetite (○)

XRD studies

X-ray diffraction (XRD) analysis was commenced using Cu $K\alpha 1$ radiation on a computer-controlled XRD machine model of X'pert pro-PANalytical. XRD patterns were recorded from 5° to 60° 2θ . The XRD peaks and analysis for raw Odaracha clay before adsorption are shown in Fig. 3. The XRD analysis of powder Odaracha clay revealed the presence of gypsum, alumina, quartz, calcite, dolomite, and magnetite. The characteristic peaks at 23.34, 29.5, 39.6, and 43.36 for the raw Odaracha sample indicated calcite (CaCO_3) as the main constituent. Some characteristic peaks at 10.62, 11.74, and 36.1 show the presence of gypsum ($\text{CaSO}_4 \cdot 2\text{H}_2\text{O}$); the peaks at 20.82 and 26.64 show the

Table 1 Effect of contact time on Cr removal efficiency ($C_0 = 110 \text{ mg/L}$, agitation speed = 150 rpm)

Contact time (min)	pH	Dose (g/L)	C_f (mg/L)	Cr adsorption %	q (mg g^{-1})
60	3	15	32.792 ± 0.095	70.189	5.147
120	3	15	26.500 ± 0.063	75.909	5.567
180	3	15	5.854 ± 0.130	94.678	6.943
240	3	15	6.896 ± 0.072	93.731	6.874

presence of quartz (SiO_2); the peak at 14.6 shows the presence of alumina (Al_2O_3); the peaks at 32 and 48.64 show the presence of dolomite ($\text{CaMg}(\text{CO}_3)_2$) and magnetite (Fe_3O_4), respectively.

Effect of various parameters on adsorption of chromium

Effect of contact time

Effect of contact time between the adsorbate and adsorbent particles is one of the important factors in the adsorption studies. To realize the effect of contact time on Cr adsorption on Odaracha adsorbent and to discern the optimum contact time between the adsorbate and adsorbent, the experiment was carried out at room temperature and led within the time range of 60–240 min in 60-min interval using 15 g/L adsorbent dose and by tuning pH of the solution at 3. Other parameters such as agitation speed and adsorbate concentration were retained constant to 150 rpm and 110 mg/L, respectively.

The result of the effect of contact time revealed in Table 1 shows that with an increase in contact time there is also an increase in percent adsorption of Cr. There was very rapid

adsorption at the initial period up to 60 min, and after that, the increase in the adsorption rate was gradual. The adsorption process attained equilibrium in 180 min, which was 94.68%. Then, no significant change in Cr removal was observed after 180 min. This is attributed to a large number of vacant surface sites which are available for adsorption during the initial stage of adsorption. As it is shown in Table 1, percentage of removal efficiency of chromium and adsorption of chromium in mg/g showed the same type of increasing trend since there was no variation of adsorbent dose in this set of experiments.

Effect of pH

The pH is a principal parameter in adsorption process because of its effect on the adsorption efficiency (Attia et al. 2010; Shahnaz et al. 2020a). The functional groups responsible for the binding of metal ions in the adsorbent surface are profoundly affected by pH. There is also a competition between ions that are present in the solution for the adsorbent’s active sites. This competition is affected by the pH of the solution (Reddy et al. 2014). The effect of pH on the adsorption process was examined by undertaking the batch procedure at 120-min contact time, under room temperature, constant agitation speed which is 150 rpm, and 15 g/L of adsorbent dosage. The investigation results on the effect of pH on chromium removal by Odaracha adsorbent are revealed in Table 2. As illustrated in Table 2, it was found that the uptake of Cr increases with decreasing pH. Accordingly, the optimum pH for the maximum uptake of chromium was pH 3. In this regard, Odaracha adsorbent gave the highest removal percentage at pH 3, which is 76.31%.

Conversely, the minimum adsorption capacity was observed at pH 6, which is 74.15%. In this experimental condition, since the adsorbent dose and initial concentration of the adsorbate had been kept constant, both adsorption percent and removal in mg/g show similar increasing trends with decreasing pH of the solution (Ajmani et al. 2019b). As per the result, the maximum chromium uptake in mg/g was detected at pH 3, which is 5.596 mg/g. At acidic pH, the dominant form of hexavalent chromium is HCrO_4^- , and at higher pH, other forms CrO_4^{2-} or $\text{Cr}_2\text{O}_7^{2-}$ predominate.

Table 2 Effect of pH on Cr removal efficiency ($C_0 = 110$ mg/L, agitation speed = 150 rpm)

pH	Contact time (min)	Dose (g/L)	C_f (mg/L)	Cr adsorption %	q (mg g ⁻¹)
3	120	15	26.063 ± 0.125	76.307	5.596
4	120	15	26.500 ± 0.063	75.909	5.567
5	120	15	28.375 ± 0.062	74.205	5.442
6	120	15	28.438 ± 0.625	74.148	5.438

Therefore, the higher adsorption capacity observed at lower pH is due to the strong electrostatic attraction between surface groups and HCrO_4^- (Singha and Das 2011; Zhu and Han 2013).

The interaction between HCrO_4^- , CrO_4^{2-} and $\text{Cr}_2\text{O}_7^{2-}$ ion and adsorbent surface decreases at higher pH because the adsorbent surface becomes negatively charged, and also there is an abundance of OH^- in aqueous solution, which can be attributed to the competitive adsorption of $\text{Cr}_2\text{O}_7^{2-}$ and OH^- . Other previous studies have also reported similar situations (Hsua et al. 2009; Owlad et al. 2010; Rangabhashiyam and Selvaraju 2015). In another way, at lower pH, the degree of surface protonation is high, so that the surface offers a maximum positive charge for adsorption of HCrO_4^- , which is predominant at lower pH. Therefore, at lower pH, the predominant hydrogen chromate ion (HCrO_4^-) requires one exchange site from Odaracha adsorbent to be adsorbed, while at higher pH, it requires two exchange sites from Odaracha adsorbent for one chromate ion (CrO_4^{2-}) adsorption (Nizam Nik Malek 2007). Generally, adsorption of chromium is higher in acidic media because at lower pH, the degree of surface protonation is very high, which plays a vital role in capturing hydrogen chromate ion (HCrO_4^-) in the solution.

Effect of adsorbent dose

As pointed out in Table 3, the effect of the dosage of Odaracha adsorbent on the removal efficiency of chromium was determined with varied adsorbent doses, which are 1 g/L, 5 g/L, 10 g/L, and 15 g/L under different experimental conditions.

As shown in Table 3, the adsorption percentage of chromium increased from 60.04 to 94.68% as the adsorbent dose increased from 1 to 15 g/L, whereas the uptake of Cr in mg/g falls from 66.042 mg/g to 6.943 mg/g when the adsorbent dose increases from 1 to 15 g/L. Higher chromium adsorption percentage with the increase in the adsorbent dose can be attributed to increasing in surface area and the availability of more binding sites for adsorption (Karthik et al. 2018; Rao et al. 2002; Reddy et al. 2014; Umoren et al. 2013). The decrease in uptake of Cr in mg/g with increased adsorbent

Table 3 Effect of adsorbent dose on Cr removal efficiency ($C_0 = 110$ mg/L, agitation speed = 150 rpm)

Dose (g/L)	pH	Contact time (min)	C_f (mg/L)	Cr adsorption %	q (mg g ⁻¹)
1	3	180	43.958 ± 0.072	60.038	66.042
5	3	180	14.667 ± 0.036	86.667	19.067
10	3	180	9.063 ± 0.063	91.761	10.094
15	3	180	5.854 ± 0.130	94.678	6.943

dose may be due to the unchanged initial concentration of metal ion and the substantial adsorption capacity of the smallest adsorbent dose or less availability of surface area per unit weight (Ajmani et al. 2019a). Similar trends have also been reported by other authors relating to the effect of adsorbent doses on adsorption efficiency of Cr (Garg et al. 2007; Ghorbani et al. 2008).

Effect of initial concentration of adsorbate

The rate of adsorption is a function of the initial concentration of adsorbate, making it a substantial factor to be considered for the optimum experimental conditions of adsorption. The effect of the various initial concentrations of chromium (30, 50, 70, 90, 110, 130, and 150 mg/L) on Cr removal efficiency at constant experimental conditions like pH 3, 180-min contact time, 150 rpm agitation speed and 15 g/L adsorbent dose is presented in Table 4.

The adsorption percentage of chromium with the various initial concentrations of adsorbate in different constant experimental conditions such as pH, contact time, agitation speed, and the adsorbent dose is presented in Table 4. According to the result exemplified in Table 4, the effect of initial concentration of Cr on the adsorption percentage shows a decreasing trend, which is 95.69, 95.33, 95.09, 94.70, 94.68, 86.88 and 83.94% with 30, 50, 70, 90, 110, 130 and 150 mg/L of adsorbate concentration, respectively. This can be explained by the fact that all adsorbents have a limited number of active sites, and at a specific concentration, the active sites become saturated (Banat et al. 2000; Tsai and Chen 2010). In another way, the reverse trend is observed in the case of Cr uptake in mg/g, which shows the increasing trend of Cr uptake, which is 1.91, 3.18, 4.44, 5.68, 6.94, 7.53, and 8.39 mg/g with increasing initial concentration of adsorbate from 30 to 150 mg/L by 20 mg/L interval. This is maybe because, at constant adsorbent dose, the number of active sites to accommodate the chromium ions remains unchanged while with rising adsorbate concentrations, the chromium ions to be accommodated increased. Therefore, the loading was faster, with a higher initial concentration of adsorbate.

Kinetic study for adsorption of chromium

To understand the rate and type of adsorption that takes place, the study applies pseudo-first-order and pseudo-second-order kinetic models.

Pseudo-first-order kinetic model

The pseudo-first-order model is expressed by Eq. (3):

$$\log(q_e - q_t) = \log q_e - \frac{k_1 t}{2.303} \tag{3}$$

where q_e and q_t (mgg⁻¹) represent the amount of Cr ions adsorbed per unit weight of the adsorbents at equilibrium and time t (min), respectively, and k_1 is the rate constant of the pseudo-first-order kinetic model.

The pseudo-first-order kinetics is applicable if the plot of $\log(q_e - q_t)$ against time (t) shows a linear relationship. In addition, the straight-line plot of $\log(q_e - q_t)$ versus t was used to determine the rate constant (k_1), q_e (cal) and the correlation coefficient (R^2). The values of k_1 and q_e (cal) in mg/g of Cr predicted from the plot shown in Fig. 4 are 4.836×10^{-2} and 49.162 mg/g, respectively. As the result presented in Table 5, the correlation coefficient ($R^2=0.5552$) indicates that

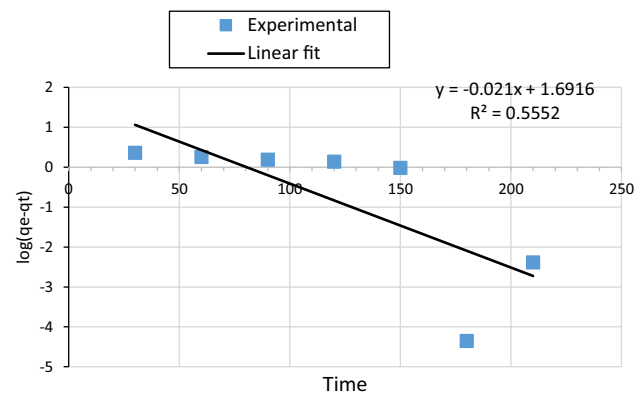


Fig. 4 Pseudo-first-order kinetics plots for the adsorption of Cr ions onto Odaracha adsorbent

Table 4 Effect of initial concentration of adsorbate on Cr removal efficiency

C_o (mg/L)	Agitation speed (rpm)	Contact time (min)	Dose (g/L)	pH	Av C_f (mg/L)	Cr adsorption%	q (mg g ⁻¹)
30	150	180	15	3	1.294 ± 0.128	95.688	1.914
50	150	180	15	3	2.333 ± 0.095	95.333	3.178
70	150	180	15	3	3.438 ± 0.062	95.089	4.438
90	150	180	15	3	4.771 ± 0.036	94.699	5.682
110	150	180	15	3	5.854 ± 0.130	94.678	6.943
130	150	180	15	3	17.063 ± 0.108	86.875	7.529
150	150	180	15	3	24.083 ± 0.072	83.944	8.394

Table 5 Line-fit model of pseudo-first- and second-order kinetics for Cr

Adsorbent	Metal	First-order			
Odaracha	Chromium	$q_e(\text{exp}) \text{ mg g}^{-1}$	$q_e(\text{cal}) \text{ mg g}^{-1}$	$k_1 \text{ (min}^{-1}\text{)}$	R^2
		6.943	49.162	4.836×10^{-2}	0.5552
Adsorbent	Metal	Second-order			
Odaracha	Chromium	$q_e(\text{exp}) \text{ mg g}^{-1}$	$q_e(\text{cal}) \text{ mg g}^{-1}$	$k_2 \text{ (g mg}^{-1}\text{min}^{-1}\text{)}$	R^2
		6.943	7.7459	3.9989×10^{-3}	0.971

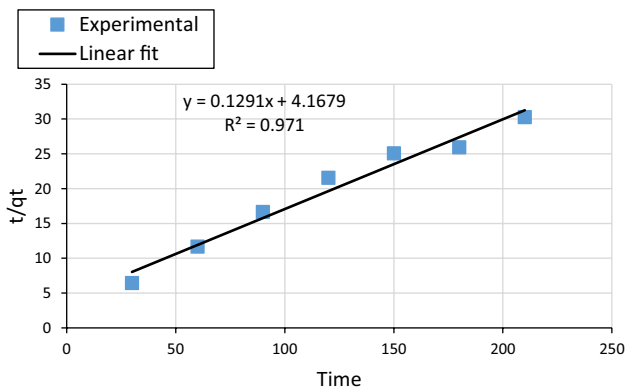


Fig. 5 Pseudo-second-order kinetics plots for the adsorption of Cr ions onto Odaracha adsorbent

the experimental data of the adsorption kinetics of chromium are not accurately supported by the pseudo-first-order model.

In a second way, the plot of $\log(q_e - q_t)$ against time (t), which is shown in Fig. 4, does not display a linear relationship, which again communicates the unsuitability of the pseudo-first-order model. Furthermore, the experimental adsorption result ($q_e(\text{exp})$) was not closer to $q_e(\text{cal})$. Therefore, the pseudo-first-order model is not suitable to explain the adsorption kinetics of Cr ions on Odaracha adsorbent (Arshadi et al. 2014; Sag and Aktay 2002).

Pseudo-second-order kinetic model

The pseudo-second-order model is expressed by Eq. (4):

$$\frac{t}{q_t} = \frac{1}{K_2 q_e^2} + \frac{t}{q_e} \tag{4}$$

where q_e and q_t (mg g^{-1}) represent the amount of Cr ions adsorbed per unit weight of the adsorbents at equilibrium and time t (min), respectively, and k_2 is the rate constant of the pseudo-second-order kinetic model. The rate constant (k_2) and calculated equilibrium adsorption capacity ($q_e(\text{cal})$) can be determined from the slope and intercept of the plot t/q_t versus t , which is shown in Fig. 5. The plot t/q_t versus t should give a straight line to apply the pseudo-second-order

kinetic model. The plot of t/q_t versus t for pseudo-second-order yields a good straight line with the highest correlation coefficient result approaching 1 ($R^2 = 0.971$). In addition, as presented in Table 5, the experimental adsorption equilibrium value ($q_e(\text{exp.}) = 6.943 \text{ mg g}^{-1}$) was well matched with the calculated adsorption equilibrium value ($q_e(\text{cal.}) = 7.745 \text{ mg g}^{-1}$). Therefore, the experimental data of the adsorption kinetics of chromium are accurately supported by a pseudo-second-order model. Thus, this finding suggests that the rate-limiting factor in the adsorption of chromium by Odaracha adsorbent is chemisorption involving the exchange of Cr ions with functional groups in the adsorbent (Rahman and Sathasivam 2015; Senthil and Gayathri, 2013).

Isotherm model for adsorption of chromium

In this study, the evaluation of the equilibrium of the adsorption process was carried out by introducing the experimental results into Langmuir and Freundlich isotherm models.

Langmuir adsorption isotherm model for chromium

Equilibrium study for the removal of chromium was performed on the Odaracha adsorbent powder by Langmuir adsorption model. According to the Langmuir isotherm model, the adsorption sites are uniformly equal and no attraction occurs between the adsorbed molecules; hence, monolayers of the molecules are deposited on the Odaracha powder (Langmuir 1916).

The linearized form of this model is presented in Eq. (5) and was used in the determination of its parameters in accordance with Fig. 6.

$$\frac{1}{q_e} = \frac{1}{q_m} + \frac{1}{q_m K_L} \cdot \frac{1}{C_e} \tag{5}$$

where q_e represents the amount of adsorbed Cr in mg/g of the adsorbent, and C_e is the concentration of Cr at equilibrium in mg/L . K_L and q_m represent Langmuir adsorption

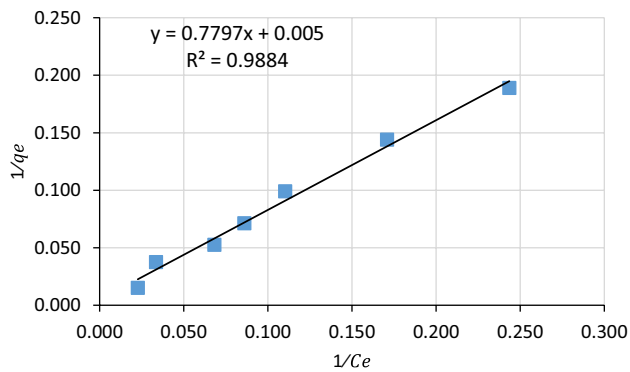


Fig. 6 Langmuir adsorption isotherm model for chromium

constant and the maximum amount of adsorbate that can be adsorbed on Odaracha adsorbent (Langmuir 1918). The values of K_L and q_m for this study were determined from the slope and intercept shown in Fig. 6. One of the essential features of this model is its ability to determine R_L as shown in Eq. (6), which is a dimensionless parameter known as equilibrium parameter or separation factor (Webber and Chakravarti 1974).

$$R_L = \frac{1}{1 + (1 + K_L + C_o)} \tag{6}$$

The adsorption process can be described as unfavorable if $R_L > 1$, linear if $R_L = 1$, favorable if $0 < R_L < 1$ and irreversible if $R_L = 0$. The value of R_L obtained in this study as presented in Table 6 is between 0 and 1, which suggests the Langmuir isotherm model is favorable in this study. The maximum monolayer coverage capacity (q_m) obtained was 200 mg g^{-1} . This result indicates that the maximum adsorption potential of 1 g of Odaracha adsorbent.

Freundlich adsorption isotherm model for Cr

The Freundlich isotherm model is an empirical equation employed to describe heterogeneous systems. In this model, it is described that during the adsorption process

different sites of the adsorbent are involved with several adsorption energy (Kumar and Kirthika 2009). The linearized form of the Freundlich isotherm model is shown in Eq. (7).

$$\log q_e = \log K_f + (1/n) \log C_e \tag{7}$$

where q_e is the metal uptake (mg g^{-1}) at equilibrium, K_f is the measure of the adsorption capacity, $1/n$ is the adsorption intensity, and C_e is the final concentration of Cr in solution, or equilibrium concentration (mg L^{-1}). The Freundlich isotherm constants K_f and $1/n$ are evaluated from the intercept and the slope, respectively, of the linear plot of $\log q_e$ versus $\log C_e$ shown in Fig. 7.

If n is between 1 and 10, it indicates favorable adsorption (Goldberg 2005). However, if $1/n$ is < 1 it indicates normal adsorption, but if it is > 1 , it implies cooperative adsorption (Mohan and Karthikeyan 1997). The numerical value of $1/n$ presented in Table 6 is 0.998, indicating a favorable adsorption process (Kannan et al. 2013).

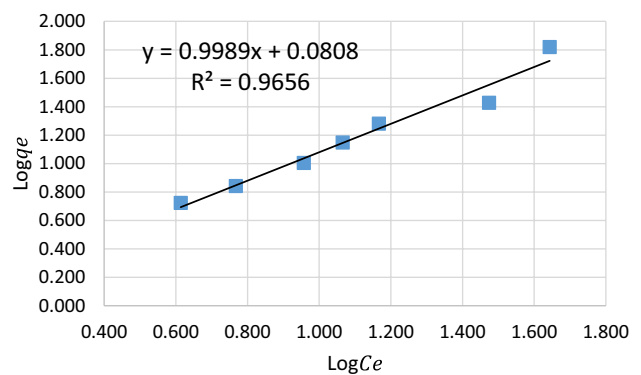


Fig. 7 Freundlich adsorption isotherm model for chromium

Table 6 Langmuir and Freundlich isotherm model constants for adsorption of Cr

Adsorbent	Metal	Langmuir			
Odaracha	Chromium	$q_m \text{ mg g}^{-1}$ 200	K_L 0.0064	R_L 0.01	R^2 0.9884
Adsorbent	Metal	Freundlich			
Odaracha	Chromium	K_f 1.2045	$1/n$ 0.998		R^2 0.9656

Table 7 Comparison between the adsorption capacities of various natural adsorbents and Odaracha soil

Type of adsorbents	Adsorption capacity q_m (mg/g)	References
Brazilian smectite	97.23	Guerra et al. (2010)
Rosehip seed shell	15.17	Şerife and Erol (2019)
Modified vermiculite	87.72	Liu et al. (2011)
Bentonite	48.83	Wanees et al. (2012)
Ziziphus jujuba cores	196.38	Labied et al. (2018)
Natural sepiolite	37	Marjanovic et al. (2013)
Odaracha soil	200	This study

Comparison of Odaracha and other natural adsorbents

A comparison results between the maximum adsorption capacity of Cr ions onto Odaracha adsorbent and other adsorbents are presented in Table 7. Table 7 shows that the maximum adsorption capacity obtained in this study was higher than other natural adsorbents illustrated in Table 7. Therefore, Odaracha soil can be used as effective and an alternative low-cost adsorbent for chromium.

Conclusions

In the exploration result of this study, Odaracha soil sourced from Saketa district of Ethiopia was used for the removal of chromium from synthetic wastewater. The characterization results of Fourier transform infrared, X-ray powder diffraction analysis, and the surface morphology of Odaracha adsorbent, which shows the pores of the surface of the adsorbent before and after adsorption, were an indicator for its adsorption capacity. The adsorption capacity of Odaracha adsorbent was influenced by a number of factors such as contact time, pH, adsorbent dosage, and initial concentration of adsorbate. The optimum range of contact time, pH, Odaracha dose, and initial concentration of chromium obtained by the batch experiment was 180 min, pH 3, 15 g/L, and 30 mg/L, respectively. With optimum experimental conditions and at room temperature, Odaracha adsorbent removed 94.68% Cr from the wastewater. The adsorption kinetics of chromium is accurately supported with a pseudo-second-order model. The isotherm data were analyzed by Langmuir and Freundlich isotherms. The maximum monolayer coverage adsorption capacity from the Langmuir adsorption isotherm model was 200 mg g⁻¹. Generally, the ability of Odaracha adsorbent in removing Cr from aqueous solutions has the potential to solve the problem of chromium-containing industrial effluents, which continue to pose increasing risks to human health and environment.

Acknowledgements The authors would like to acknowledge both Addis Ababa University, Center of Environmental Science and Jigjiga University for their holistic support including financial aid.

Author contributions YB contributed to experimental design, conducting experiments, analyzed and interpreted the data, and wrote the manuscript. SL contributed to the experimental design, supervising the whole research work, and editing the manuscript. GA involved in the characterization of the adsorbent material and editing the manuscript.

Funding This research was financially supported by Addis Ababa University and Jigjiga University.

Data Availability The authors declare that the data supporting the findings of this study are available within the article, and other supplementary data are available from the corresponding author upon request.

Compliance with ethical standards

Conflict of interest The authors declare that they have no conflict of interests.

Ethical approval Not applicable.

Consent for publication Not applicable.

Open Access This article is licensed under a Creative Commons Attribution 4.0 International License, which permits use, sharing, adaptation, distribution and reproduction in any medium or format, as long as you give appropriate credit to the original author(s) and the source, provide a link to the Creative Commons licence, and indicate if changes were made. The images or other third party material in this article are included in the article's Creative Commons licence, unless indicated otherwise in a credit line to the material. If material is not included in the article's Creative Commons licence and your intended use is not permitted by statutory regulation or exceeds the permitted use, you will need to obtain permission directly from the copyright holder. To view a copy of this licence, visit <http://creativecommons.org/licenses/by/4.0/>.

References

- Ajmani A, Shahnaz T, Narayanan S, Narayanasamy S (2019a) Equilibrium, kinetics and thermodynamics of hexavalent chromium biosorption on pristine and zinc chloride activated Senna siamea seed pods. *Chem Ecol* 35(4):379–396. <https://doi.org/10.1080/02757540.2019.1584614>
- Ajmani A, Shahnaz T, Subbiah S, Narayanasamy S (2019b) Hexavalent chromium adsorption on virgin, biochar, and chemically modified carbons prepared from Phanera vahlii fruit biomass: equilibrium, kinetics, and thermodynamics approach. *Environ Sci Pollut Res* 26:32137–32150
- Arshadi M, Amiri M, Mousavi S (2014) Kinetic, equilibrium and thermodynamic investigations of Ni(II), Cd(II), Cu(II) and Co(II) adsorption on barley straw ash. *Water Resour Ind* 6:1–17
- Attia A, Khedr S, Elkholy S (2010) Adsorption of chromium ion (VI) by acid activated carbon. *Braz J Chem Eng* 27(1):183–193
- Banat FA, Al-Bashir B, Al-Asheh S, Hayajneh O (2000) Adsorption of phenol by bentonite. *Environ Pollut* 107:391–398
- Costanzo F, Silvestrelli PL, Ancilotto F (2012) Physisorption, diffusion and chemisorbed pathways of H₂ molecule on Graphene and

- single walled nanotube by first principle calculations. *J Chem Theory Comput* 8(4):1288–1294
- Dagmawi M, Mekibib D (2013) Chromium removal from modjo tannery wastewater using moringa stenopetala seed powder as an adsorbent. *Water, Air, & Soil Pollut* 224(12):1–10
- Eliku T, Leta S (2018) Spatial and seasonal variation in physicochemical parameters and heavy metals in Awash River, Ethiopia. *Appl Water Sci* 8:177. <https://doi.org/10.1007/s13201-018-0803-x>
- Garg UK, Kaur MP, Garg VK, Sud D (2007) Removal of hexavalent chromium from aqueous solution by agricultural waste biomass. *Hazard Mater* 140:60–68
- Ghoneim M, El-Desoky H, El-Moselhy K, Amer A, ElNaga E, Mohamedein L, Al-Prol A (2014) Removal of cadmium from aqueous solution using marie green algae, *Ulvalactuca* Egypt. *J Aquat Res* 40:235–242
- Ghorbani F, Younesi H, Ghasempouri SM, Zinatizadeh AA, Amini M, Daneshi A (2008) Application of response surface methodology for optimization of cadmium biosorption in an aqueous solution by *Saccharomyces cerevisiae*. *Chem Eng J* 145(2):267–275
- Goldberg S (2005) Equations and models describing adsorption processes in soils. SSSA Book, Soil Science Society of American, USA
- Guerra DL, Oliveira HC, da Costa CP, Viana RR, Airoidi C (2010) Adsorption of chromium (VI) ions on Brazilian smectite: effect of contact time, pH, concentration, and calorimetric investigation. *CATENA* 82:35–44
- Gulipalli CS, Prasad B, Wasewar KL (2011) Batch study, equilibrium and kinetics of adsorption of selenium using rice husk ash (RHA). *J Eng Sci Technol* 6:586–605
- Hoidy W, Ahmed B, Ibrahim N (2009) Synthesis and characterization of organo clay from soidium montmorillonite and fatty hydroxamic acid. *J Appl Sci* 6(8):167–172
- Hsua NH, Wanga YH, Liaoa HST, Tzoua YM, Huang YM (2009) Removal of hexavalent chromium from acidic aqueous solutions using rice straw-derived carbon. *J Hazard Mater* 171:1066–1070
- Jiang W, Pelaez M, Dionysiou DD, Entezari MH, Tsoutsou D, O'Shea K (2013) Chromium (VI) removal by maghemite nanoparticles. *Chem Eng J* 222:527–533
- Kannan C, Muthuraja K, Devi M (2013) Hazardous dyes removal from aqueous solution over mesoporous aluminophosphate with textural porosity by adsorption. *J Hazard Mater* 244(245):10–20
- Karthik V, Saravanan K, Patra C, Ushadevi B, Vairam S, Selvaraju N (2018) Biosorption of Acid Yellow 12 from simulated wastewater by non-viable *T. harzianum*: kinetics, isotherm and thermodynamic studies. *Int J Environ Sci Technol*. <https://doi.org/10.1007/s13762-018-2073-4>
- Kumar PS, Kirthika K (2009) Equilibrium and kinetic study of adsorption of nickel from aqueous solution onto bael tree leaf powder. *J Eng Sci Technol* 4(4):351–363
- Kyziol-Komosinska J, Rosik-Dulewska C, Dzieniszewska A, Pajak M, Krzyzewska I (2014) Removal of Cr (III) ions from water and wastewater by sorption onto peats clays occurring in an overburden of lignite beds in Central Poland. *Environ Protect Eng* 40(1):5–22. <https://doi.org/10.5277/epe140101>
- Labied R, Benturki O, Hamitouche AE, Donnot A (2018) Adsorption of hexavalent chromium by activated carbon obtained from a waste lignocellulosic material (*Ziziphus jujuba* cores): kinetic, equilibrium, and thermodynamic study. *Adsorp Sci Technol* 36(3–4):1066–1099. <https://doi.org/10.1177/0263617417750739>
- Langmuir I (1916) The construction and fundamental properties of solids and liquids. Part I. Solids *J Am Chem Soc* 38:2221–2295
- Langmuir I (1918) The adsorption of gases on plane surfaces of glass, mica and platinum. *J Am Chem Soc* 40:1361–1403
- Liu Y, Li H, Tan GQ, Zhu XH (2011) Fe²⁺ modified vermiculite for the removal of chromium (VI) from aqueous solution. *Sep Sci Technol* 46:290–299
- Malek NANN (2007) Surfactant modified zeolite Y as a sorbent for some chromium and arsenic species in water. Universiti Teknologi Malaysia
- Marjanovic V, Lazarevic S, Jankovic-Castvan I, Jokic B, Janackovic DJ, Petrovic R (2013) Adsorption of chromium (VI) from aqueous solutions onto amine functionalized natural and acid-activated sepiolites. *Appl Clay Sci* 80–81:202–210
- Mohan S, Karthikeyan J (1997) Removal of lignin and tannin color from aqueous solution by adsorption onto activated charcoal. *Environ Pollut* 97:183–187
- Ofudje E, Awotula A, Oladipo G, Williams O (2014) Detoxification of chromium (VI) ions in aqueous solution via adsorption by raw and activated Carbon prepared from sugarcane bio waste. *Covenant J Phys Life Sci* 2:110–122
- Owlad M, Aroua MK, Daud WM (2010) Hexavalent chromium adsorption on impregnated palm shell activated carbon with polyethyleneimine. *Bioresour Technol* 101:5098–5103. <https://doi.org/10.1016/j.biortech.2010.01.135>
- Pranay AR, Anup C, Yogesh M (2015) Various techniques for the removal of Chromium and lead from waste water: review. *Int J Emerg Trends Eng Basic Sci (IJEEBS)* 2(2):64–67
- Rahman MS, Sathasivam KV (2015) Heavy metal adsorption onto *Kappaphycus* sp. from aqueous solutions: the use of error functions for validation of isotherm and kinetics models. Hindawi Publishing Corporation, BioMed Research International 1–13.
- Rangabhashiyam S, Selvaraju N (2015) Adsorptive remediation of hexavalent chromium from synthetic wastewater by a natural and ZnCl₂ activated *Sterculia guttata* shell. *J Mol Liq* 207:39–49
- Rao M, Parwate AV, Bhole AG (2002) Removal of Cr⁶⁺ and Ni²⁺ from aqueous solution using bagasse and fly ash. *Waste Manag* 22:821–830
- Reddy NA, Lakshmi pathy R, Sarada NC (2014) Application of *Citrus lanatus* rind as biosorbent for removal of trivalent chromium from aqueous solution. *Alexandria Eng J* 53(4):969–975
- Sag Y, Aktay F (2002) Kinetic studies on sorption of Cr (VI) and Cu (II) ions by chitin, chitosan and *Rhizopus arrhizus*. *Biochem Eng J* 1(12):143–153
- Senthil K, Gayathri J (2013) Adsorption of Pb²⁺ ions from aqueous solutions onto bael tree leaf powder: isotherms, kinetics and thermodynamics study. *J Chem Eng Sci Technol* 4(4):381–399
- Şerife P, Erol P (2019) Comparative study of Cr(VI) removal by bio-waste adsorbents: equilibrium, kinetics, and thermodynamic. *J Anal Sci Technol* 10:15. <https://doi.org/10.1186/s40543-019-0175-3>
- Shahnaz T, Mohamed Madhar Fazil S, Padmanaban VC, Narayanasamy S (2020a) Surface modification of nanocellulose using polypyrrole for the adsorptive removal of Congo red dye and chromium in binary mixture. *Int J Biol Macromol* 151:322–332
- Shahnaz T, Sharma V, Subbiah S, Narayanasamy S (2020b) Multivariate optimisation of Cr (VI), Co (III) and Cu (II) adsorption onto nanobentonite incorporated nanocellulose/chitosan aerogel using response surface methodology. *J Water Process Eng* 36:101283
- Singha B, Das SK (2011) Biosorption of Cr (VI) ions from aqueous solutions: kinetics, equilibrium, thermodynamics and desorption studies. *Colloids Surf, B* 84:221–232
- Tsai WT, Chen HR (2010) Removal of malachite green from aqueous solution using low-cost chlorella-based biomass. *J Hazard Mater* 175(1):844–849
- Umoren SA, Etim UJ, Israel AU (2013) Adsorption of methylene blue from industrial effluent using poly(vinyl alcohol). *J Mater Environ Sci* 4:75–86
- Wanees SA, Ahmed AM, Adam MS, Mohamed MW (2012) Adsorption studies on the removal of hexavalent chromium-contaminated wastewater using activated carbon and bentonite. *Chem J* 2:95–105

- Webber TN, Chakravarti RK (1974) Pore and solid diffusion models for fixed bed adsorbers. *AIChE J* 20:228–238
- Zhu X, Han B (2013) Adsorption behavior of chromium (VI) on the HDTMA-modified- zeolite. *J Food Agric Environ* 11(3):2488–2492

Publisher's Note Springer Nature remains neutral with regard to jurisdictional claims in published maps and institutional affiliations.